the transcriptional repression by wild-type PAX5 but did not affect that by mutant PAX5 and diminished the difference between them (Supplemental Fig. 2C).

BCR signal-induced PAX5 phosphorylation increased BLIMP1 expression in B cells

To further confirm the BLIMP1 derepression by BCR stimulation, we first examined BLIMP1 mRNA expression after BCR stimulation in Ramos cells. BLIMP1 mRNA expression was induced by BCR stimulation following ERK1/2 and PAX5 phosphorylation, and U0126 inhibited the induction of BLIMP1 expression (Fig. 4A). Next, we used Ramos transfectants with specific knockdown of endogenous PAX5. Exogenous expression of wild-type and mutant PAX5 reduced BLIMP1 expression. BCR stimulation relieved BLIMP1 repression by wild-type PAX5, whereas repression by mutant PAX5 was resistant to BCR stimulation (Fig. 4B). These data indicated that BCR signal-induced BLIMP1 expression was mediated by PAX5 phosphorylation by ERK1/2. Notably, in contrast to the luciferase assay in Fig. 3B, no difference in the repression of BLIMP1 was observed between wild-type and mutant PAX5 transfectants of Ramos cells when there was no BCR stimulation (Fig. 4B, *lane 3* versus *lane 5*). This occurs because Ramos cells have no constitutive ERK1/2 activation, which is different from 293T cells (Supplemental Fig. 2B).

We also examined BCR signal-induced BLIMP1 expression in mouse spleen B cells. BCR stimulation of mouse spleen B cells induced BLIMP1 mRNA expression, which was inhibited by U0126 (Fig. 4C). Taken together with BCR signal-induced PAX5 phosphorylation in these cells (Fig. 2D), these data implied that BCR signal-induced BLIMP1 derepression through PAX5 phosphorylation by ERK1/2 might also occur in primary B cells.

PAX5 phosphorylation did not affect DNA-binding ability or cellular localization

To clarify how PAX5 phosphorylation attenuated its function, we used EMSA to investigate the effect of PAX5 phosphorylation on DNA-binding ability. PAX5, synthesized in vitro, was incubated with radiolabeled oligomers containing the PAX5-binding sequence in the *CD19* promoter. The obtained single band was competed by the presence of a 200-fold molar excess of non-radiolabeled oligomers and was supershifted by anti-PAX5 Ab but not by control rabbit IgG (Fig. 5A). Wild-type and mutant PAX5 were subjected to in vitro kination, with or without ERK2, and then to EMSA. No difference in DNA-binding activity was observed, regardless of phosphorylation by ERK2 and phosphorylation-defective mutation (Fig. 5A). These results indicated that PAX5 phosphorylation did not affect its DNA-binding ability.

Next, we examined the alteration of PAX5 cellular localization by coexpression of CA-MEK1 or phosphorylation-defective mutation. Overexpressed wild-type and mutant PAX5 localized diffusely in the nucleus, and this was not affected by coexpression of CA-MEK1, suggesting that cellular localization of PAX5 was not altered by its phosphorylation (Fig. 5B). The molecular mecha-

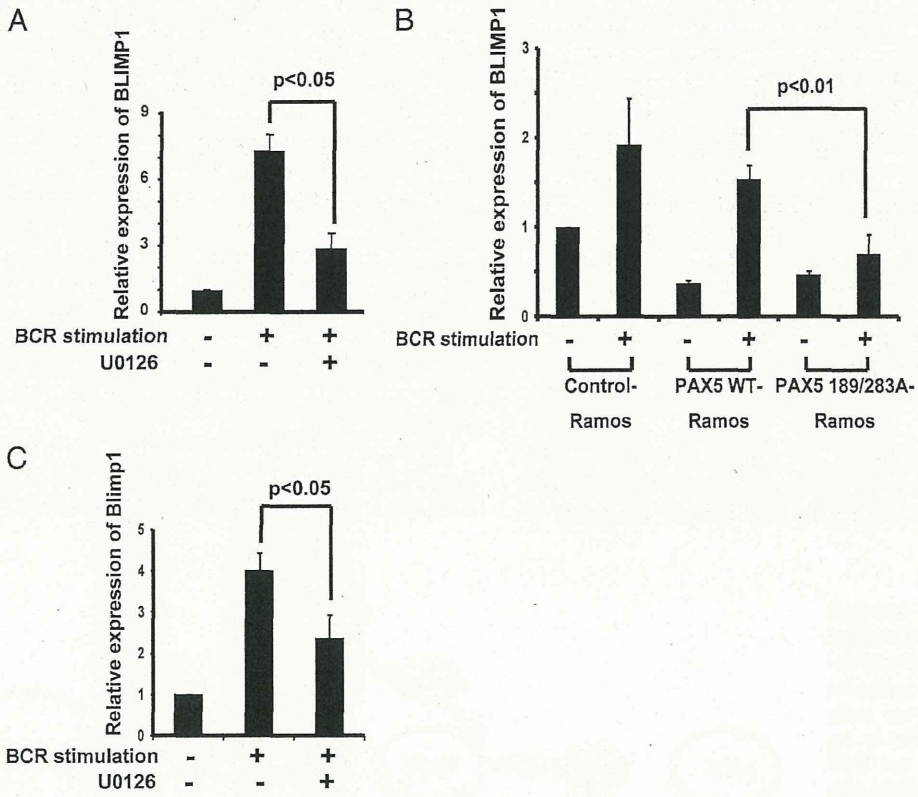

FIGURE 4. PAX5 phosphorylation plays an important role in BCR signal-induced BLIMP1 expression. (**A**) MEK1 inhibitor inhibited BCR signal-induced BLIMP1 expression. Ramos cells were treated as in Fig. 2A. Eight hours after stimulation, RNA was harvested, and mRNA expression of BLIMP1 was quantified by real-time RT-PCR. The relative mRNA expression levels reflect duplicate values from two independent experiments. Statistical comparisons were performed by using the *t* test. (**B**) Phosphorylation-defective mutant of PAX5 abolished BCR signal-induced BLIMP1 expression. Control-Ramos, PAX5 Wild-Ramos, and PAX5 189/283A-Ramos cells were introduced siRNA for specific knockdown of endogenous PAX5 and stimulated with anti-IgM Ab for BCR stimulation as in Fig. 2C. RNA harvest and quantification of BLIMP1 mRNA were performed as in (A). (**C**) MEK1 inhibitor inhibited BCR signal-induced BLIMP1 expression in mouse spleen B cells. Mouse spleen B cells, purified as described in *Materials and Methods*, were treated and analyzed as in (A), except that cells were stimulated with anti-IgM Ab (10 μg/ml), and RNA extraction was performed 1 h after stimulation.

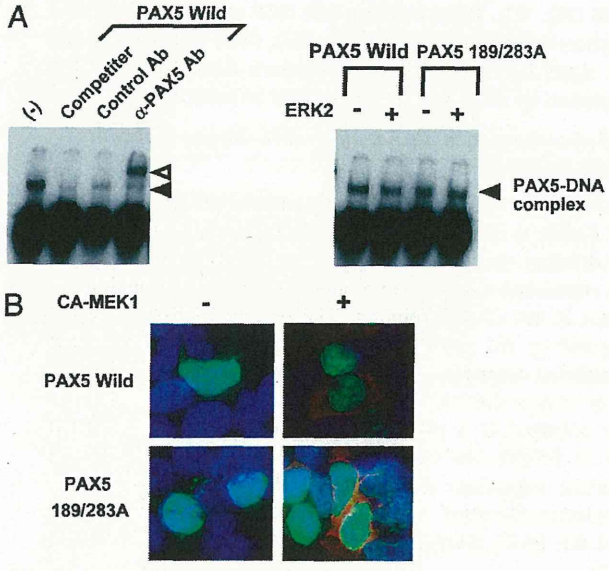

FIGURE 5. PAX5 phosphorylation did not affect DNA-binding ability or cellular localization. (**A**) Phosphorylation of PAX5 did not affect DNA-binding ability. Equal amounts of PAX5 synthesized in vitro were incubated with ^{32}P-labeled oligonucleotide probe containing the PAX5-binding sequence of the *CD19* promoter in the presence or absence of a 200-fold molar excess of unlabeled oligonucleotide (competitor), normal rabbit IgG (control Ab), or anti-PAX5 Ab (*left panel*). PAX5–DNA complex (black arrowhead) was visualized with an imaging analyzer. Supershifted band is indicated by the white arrowhead. Equal amounts of wild-type and mutant PAX5 were first subjected to in vitro phosphorylation, with or without ERK2, and then applied to EMSA (*right panel*). DNA-binding ability of PAX5 was not affected by phosphorylation. (**B**) Phosphorylation of PAX5 did not affect its localization. 293T cells were transfected with the expression vectors for wild-type and mutant PAX5, with or without HA-tagged CA-MEK1. Localization of PAX5 was observed with immunofluorescence staining using anti-PAX5 Ab with Alexa Fluor 488-conjugated secondary Ab (green), anti-HA Ab with Alexa Fluor 568-conjugated secondary Ab (red), and DAPI (blue). Original magnification ×400. Diffuse nuclear localization of PAX5 was not affected by the coexpression of HA-tagged CA-MEK1 or phosphorylation site mutations.

nisms through which PAX5 phosphorylation abolishes transcriptional repression of BLIMP1 are unknown.

Discussion

The data presented in this article support our speculation that PAX5 phosphorylation by ERK1/2 negatively affected BLIMP1 repression by PAX5. It is reported that BLIMP1 repression by PAX5 is abolished after BCR stimulation by Ag. Once BLIMP1 is expressed, it suppresses PAX5, which allows greater expression of BLIMP1. This positive feedback loop enables quick replacement of PAX5 with BLIMP1, which initiates plasma cell differentiation (14). Kallies et al. (16) investigated the first event of plasma cell differentiation in detail; they reported that the abolition of PAX5-mediated repression of BLIMP1 was the first event to initiate plasma cell differentiation and that the mechanism was neither a decrease in the DNA-binding ability of PAX5 nor downregulation of the PAX5 expression level and was yet to be revealed. PAX5 phosphorylation by ERK1/2 could be a clue to this uncertainty. The schema of this putative model is shown in Fig. 6.

It should be noted that Ramos cells or primary B cells from mouse spleen did not undergo plasma cell differentiation as the result of BCR stimulation with anti-IgM Ab (data not shown), despite the stimulation-induced phosphorylation of ERK1/2 and PAX5 and BLIMP1 expression. We could not keep the primary B cells alive for longer than a few days and could not estimate the differentiation. With regard to Ramos cells, one possible reason is that ERK1/2 phosphorylation induced by anti-IgM Ab stimulation was transient, peaking 10 min after stimulation and returning to basal levels ~2 h later. The kinetics of PAX5 phosphorylation were similar to those of ERK1/2 phosphorylation and, consistent with these kinetics, BLIMP1 mRNA expression was also transient and returned to the basal level within 24 h (data not shown). After anti-IgM Ab stimulation, BLIMP1 expression in Ramos cells is not sufficient to suppress PAX5 and initiate the above-described positive-feedback loop to replace PAX5 with BLIMP1. BCR stimulation with Ag is not the only stimulation required for plasma cell differentiation. Stimulation with cytokines, such as IL-2, IL-4, IL-10, and IL-21, and contact-dependent engagement of CD40 on B cells by CD40L (CD154), expressed by activated CD4$^+$ T cells, are required for plasma differentiation (22–26). Costimulation with these cytokines and T cells might prolong and enhance ERK1/2 phosphorylation and PAX5 phosphorylation and enable enough BLIMP1 expression to initiate plasma cell differentiation. The other possible reason is that Ramos cells, a lymphoma cell line, have impaired differentiation, as do tumor cells. BLIMP1 expression is induced by the cooperation of transcription factors, such as STAT3, IRF-4, and NF-κB (27, 28). Normal GCB cells express these factors properly and are ready to respond to BCR stimulation, which might enable a rapid and substantial increase in BLIMP1 expression in response to even transient PAX5 phosphorylation.

Other researchers reported the phosphorylation of PAX family proteins by the MAPK superfamily. PAX2 is phosphorylated by JNK at the transactivation domain (29), and both ERK1/2 and

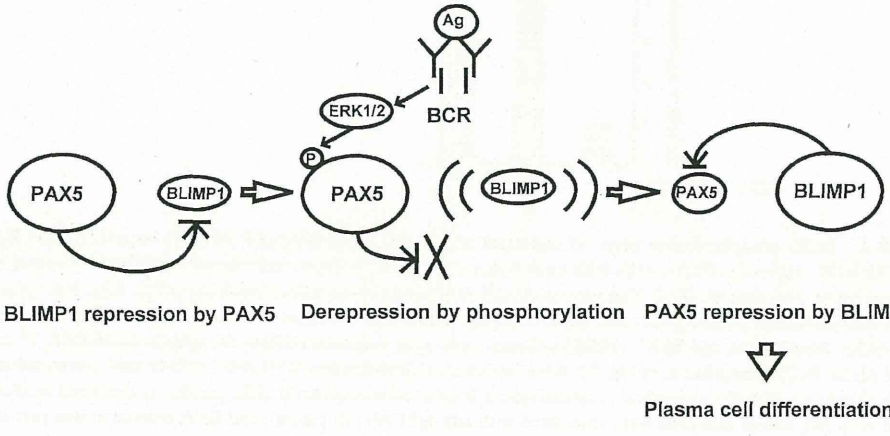

FIGURE 6. Putative schematic model of plasma cell differentiation triggered by PAX5 phosphorylation. PAX5 represses BLIMP1 expression during B cell development (*left*). When BCR signal is induced by Ag, ERK1/2 signal activation and PAX5 phosphorylation occur simultaneously, and repression of BLIMP1 is attenuated by PAX5 phosphorylation (*middle*). Once BLIMP1 is expressed, it suppresses PAX5 (*right*). Finally, PAX5 is replaced with BLIMP1, and plasma cell differentiation is initiated.

p38 phosphorylate PAX6 at the same sites: serines 376 and 413 and threonine 323 (30). This phosphorylation enhances the transcriptional activities of PAX family proteins. In addition, PAX6 phosphorylation by homeodomain-interacting protein kinase 2 (31), sumoylation of PAX6 (32), and acetylation of PAX5 by p300 (33) are reported to be posttranslational modifications of PAX family proteins, and all enhance the transactivation of PAX family proteins; therefore, negative regulation of PAX5 function by phosphorylation seems to be unique. Serines of PAX5 phosphorylation sites are not conserved in any other PAX family proteins. PAX5 is the only PAX family protein that regulates the differentiation of hematopoietic cells and might obtain a unique method to respond to extracellular signals. Furthermore, the cancellation of PAX family-dependent transcriptional repression by phosphorylation may also be unique to PAX5, although the effect of phosphorylation on transcriptional repression by other members of the PAX family has not been investigated.

The aberrant expression of normal PAX5 protein by the fusion gene between the potent enhancer of the *IGH* gene and the *PAX5* promoter was found in non-Hodgkin's lymphoma patients with the chromosomal translocation, t(9;14)(p13;q32) (34, 35). The oncogenicity of this fusion gene might be explained by impaired initiation of plasma cell differentiation due to sustained repression of BLIMP1 by overexpressed PAX5. Similarly, phosphorylation-defective mutation of PAX5 might impair plasma cell differentiation and cause lymphoma; therefore, we examined the genome DNA sequence surrounding PAX5 phosphorylation sites in 85 cases of diffuse large B cell lymphoma, but no mutation was found (data not shown; information on samples and sequencing methods is described in *Materials and Methods*). PAX5 mutations in lymphoma cells, if they exist, might be at the ERK1/2 binding site of PAX5, which is currently unknown.

In summary, our study provides evidence for an ERK1/2 pathway that phosphorylates PAX5 in response to BCR stimulation; this increase in PAX5 phosphorylation may associate with attenuated transcriptional repression by PAX5, derepression of BLIMP1, and initiation of plasma cell differentiation. This work provides new insight into the regulation of PAX5 function and establishes a novel relationship among the BCR signal, ERK1/2, and PAX5.

Acknowledgments

We thank Tomoko Kawake, Yoko Matsuyama, Asako Watanabe, and Chika Wakamatsu for technical assistance.

Disclosures

T.N. received research funding from Otsuka Pharmaceutical Co., Ltd., Kyowa Hakko Kirin Co., Ltd., Wyeth, and Chugai Pharmaceutical Co., Ltd. K.S. is a graduate student at Nagoya University and an employee of Otsuka Pharmaceutical Co., Ltd.

References

1. Nutt, S. L., A. M. Morrison, P. Dörfler, A. Rolink, and M. Busslinger. 1998. Identification of BSAP (Pax-5) target genes in early B-cell development by loss- and gain-of-function experiments. *EMBO J.* 17: 2319–2333.
2. Busslinger, M. 2004. Transcriptional control of early B cell development. *Annu. Rev. Immunol.* 22: 55–79.
3. Mikkola, I., B. Heavey, M. Horcher, and M. Busslinger. 2002. Reversion of B cell commitment upon loss of Pax5 expression. *Science* 297: 110–113.
4. Nutt, S. L., D. Eberhard, M. Horcher, A. G. Rolink, and M. Busslinger. 2001. Pax5 determines the identity of B cells from the beginning to the end of B-lymphopoiesis. *Int. Rev. Immunol.* 20: 65–82.
5. Kozmik, Z., S. Wang, P. Dörfler, B. Adams, and M. Busslinger. 1992. The promoter of the CD19 gene is a target for the B-cell-specific transcription factor BSAP. *Mol. Cell. Biol.* 12: 2662–2672.
6. Maier, H., R. Ostraat, S. Parenti, D. Fitzsimmons, L. J. Abraham, C. W. Garvie, and J. Hagman. 2003. Requirements for selective recruitment of Ets proteins and activation of mb-1/Ig-alpha gene transcription by Pax-5 (BSAP). *Nucleic Acids Res.* 31: 5483–5489.
7. Schebesta, M., P. L. Pfeffer, and M. Busslinger. 2002. Control of pre-BCR signaling by Pax5-dependent activation of the BLNK gene. *Immunity* 17: 473–485.
8. Morrison, A. M., S. L. Nutt, C. Thévenin, A. Rolink, and M. Busslinger. 1998. Loss- and gain-of-function mutations reveal an important role of BSAP (Pax-5) at the start and end of B cell differentiation. *Semin. Immunol.* 10: 133–142.
9. Souabni, A., C. Cobaleda, M. Schebesta, and M. Busslinger. 2002. Pax5 promotes B lymphopoiesis and blocks T cell development by repressing Notch1. *Immunity* 17: 781–793.
10. Holmes, M. L., S. Carotta, L. M. Corcoran, and S. L. Nutt. 2006. Repression of Flt3 by Pax5 is crucial for B-cell lineage commitment. *Genes Dev.* 20: 933–938.
11. Usui, T., Y. Wakatsuki, Y. Matsunaga, S. Kaneko, H. Koseki, and T. Kita. 1997. Overexpression of B cell-specific activator protein (BSAP/Pax-5) in a late B cell is sufficient to suppress differentiation to an Ig high producer cell with plasma cell phenotype. [Published erratum appears in 1999 *J. Immunol.* 163: 1091.] *J. Immunol.* 158: 3197–3204.
12. Reimold, A. M., P. D. Ponath, Y. S. Li, R. R. Hardy, C. S. David, J. L. Strominger, and L. H. Glimcher. 1996. Transcription factor B cell lineage-specific activator protein regulates the gene for human X-box binding protein 1. *J. Exp. Med.* 183: 393–401.
13. Wang, L. D., and M. R. Clark. 2003. B-cell antigen-receptor signalling in lymphocyte development. *Immunology* 110: 411–420.
14. Lin, K. I., C. Angelin-Duclos, T. C. Kuo, and K. Calame. 2002. Blimp-1-dependent repression of Pax-5 is required for differentiation of B cells to immunoglobulin M-secreting plasma cells. *Mol. Cell. Biol.* 22: 4771–4780.
15. Calame, K. L., K. I. Lin, and C. Tunyaplin. 2003. Regulatory mechanisms that determine the development and function of plasma cells. *Annu. Rev. Immunol.* 21: 205–230.
16. Kallies, A., J. Hasbold, K. Fairfax, C. Pridans, D. Emslie, B. S. McKenzie, A. M. Lew, L. M. Corcoran, P. D. Hodgkin, D. M. Tarlinton, and S. L. Nutt. 2007. Initiation of plasma-cell differentiation is independent of the transcription factor Blimp-1. *Immunity* 26: 555–566.
17. Kurahashi, S., F. Hayakawa, Y. Miyata, T. Yasuda, Y. Minami, S. Tsuzuki, A. Abe, and T. Naoe. 2011. PAX5-PML acts as a dual dominant-negative form of both PAX5 and PML. *Oncogene* 30: 1822–1830.
18. Hayakawa, F., and M. L. Privalsky. 2004. Phosphorylation of PML by mitogen-activated protein kinases plays a key role in arsenic trioxide-mediated apoptosis. *Cancer Cell* 5: 389–401.
19. Morgan, M. A., E. Magnusdottir, T. C. Kuo, C. Tunyaplin, J. Harper, S. J. Arnold, K. Calame, E. J. Robertson, and E. K. Bikoff. 2009. Blimp-1/Prdm1 alternative promoter usage during mouse development and plasma cell differentiation. *Mol. Cell. Biol.* 29: 5813–5827.
20. Hayakawa, F., M. Towatari, Y. Ozawa, A. Tomita, M. L. Privalsky, and H. Saito. 2004. Functional regulation of GATA-2 by acetylation. *J. Leukoc. Biol.* 75: 529–540.
21. Yasuda, T., K. Kometani, N. Takahashi, Y. Imai, Y. Aiba, and T. Kurosaki. 2011. ERKs induce expression of the transcriptional repressor Blimp-1 and subsequent plasma cell differentiation. *Sci. Signal.* 4: ra25.
22. Splawski, J. B., D. F. Jelinek, and P. E. Lipsky. 1989. Immunomodulatory role of IL-4 on the secretion of Ig by human B cells. *J. Immunol.* 142: 1569–1575.
23. Kuchen, S., R. Robbins, G. P. Sims, C. Sheng, T. M. Phillips, P. E. Lipsky, and R. Ettinger. 2007. Essential role of IL-21 in B cell activation, expansion, and plasma cell generation during CD4+ T cell-B cell collaboration. *J. Immunol.* 179: 5886–5896.
24. Jelinek, D. F., J. B. Splawski, and P. E. Lipsky. 1986. The roles of interleukin 2 and interferon-gamma in human B cell activation, growth and differentiation. *Eur. J. Immunol.* 16: 925–932.
25. Itoh, K., T. Inoue, K. Ito, and S. Hirohata. 1994. The interplay of interleukin-10 (IL-10) and interleukin-2 (IL-2) in humoral immune responses: IL-10 synergizes with IL-2 to enhance responses of human B lymphocytes in a mechanism which is different from upregulation of CD25 expression. *Cell. Immunol.* 157: 478–488.
26. Good, K. L., V. L. Bryant, and S. G. Tangye. 2006. Kinetics of human B cell behavior and amplification of proliferative responses following stimulation with IL-21. *J. Immunol.* 177: 5236–5247.
27. Kwon, H., D. Thierry-Mieg, J. Thierry-Mieg, H. P. Kim, J. Oh, C. Tunyaplin, S. Carotta, C. E. Donovan, M. L. Goldman, P. Tailor, et al. 2009. Analysis of interleukin-21-induced Prdm1 gene regulation reveals functional cooperation of STAT3 and IRF4 transcription factors. *Immunity* 31: 941–952.
28. Johnson, K., M. Shapiro-Shelef, C. Tunyaplin, and K. Calame. 2005. Regulatory events in early and late B-cell differentiation. *Mol. Immunol.* 42: 749–761.
29. Cai, Y., M. S. Lechner, D. Nihalani, M. J. Prindle, L. B. Holzman, and G. R. Dressler. 2002. Phosphorylation of Pax2 by the c-Jun N-terminal kinase and enhanced Pax2-dependent transcription activation. *J. Biol. Chem.* 277: 1217–1222.
30. Mikkola, I., J. A. Bruun, G. Bjorkoy, T. Holm, and T. Johansen. 1999. Phosphorylation of the transactivation domain of Pax6 by extracellular signal-regulated kinase and p38 mitogen-activated protein kinase. *J. Biol. Chem.* 274: 15115–15126.
31. Kim, E. A., Y. T. Noh, M. J. Ryu, H. T. Kim, S. E. Lee, C. H. Kim, C. Lee, Y. H. Kim, and C. Y. Choi. 2006. Phosphorylation and transactivation of Pax6 by homeodomain-interacting protein kinase 2. *J. Biol. Chem.* 281: 7489–7497.
32. Yan, Q., L. Gong, M. Deng, L. Zhang, S. Sun, J. Liu, H. Ma, D. Yuan, P. C. Chen, X. Hu, et al. 2010. Sumoylation activates the transcriptional activity of Pax-6, an important transcription factor for eye and brain development. *Proc. Natl. Acad. Sci. USA* 107: 21034–21039.

33. He, T., S. Y. Hong, L. Huang, W. Xue, Z. Yu, H. Kwon, M. Kirk, S. J. Ding, K. Su, and Z. Zhang. 2011. Histone acetyltransferase p300 acetylates Pax5 and strongly enhances Pax5-mediated transcriptional activity. *J. Biol. Chem.* 286: 14137–14145.
34. Iida, S., P. H. Rao, P. Nallasivam, H. Hibshoosh, M. Butler, D. C. Louie, V. Dyomin, H. Ohno, R. S. Chaganti, and R. Dalla-Favera. 1996. The t(9;14)(p13;q32) chromosomal translocation associated with lymphoplasmacytoid lymphoma involves the PAX-5 gene. *Blood* 88: 4110–4117.
35. Busslinger, M., N. Klix, P. Pfeffer, P. G. Graninger, and Z. Kozmik. 1996. Deregulation of PAX-5 by translocation of the Emu enhancer of the IgH locus adjacent to two alternative PAX-5 promoters in a diffuse large-cell lymphoma. *Proc. Natl. Acad. Sci. USA* 93: 6129–6134.

Dendritic Cell-Specific Ablation of the Protein Tyrosine Phosphatase Shp1 Promotes Th1 Cell Differentiation and Induces Autoimmunity

Tetsuya Kaneko,*,†,1 Yasuyuki Saito,*,‡,1 Takenori Kotani,*,1 Hideki Okazawa,*,§ Hiroko Iwamura,* Miho Sato-Hashimoto,* Yoshitake Kanazawa,* Satoshi Takahashi,‡ Keiju Hiromura,‡ Shinya Kusakari,* Yoriaki Kaneko,‡ Yoji Murata,*,§ Hiroshi Ohnishi,* Yoshihisa Nojima,‡ Kenji Takagishi,† and Takashi Matozaki*,§

Dendritic cells (DCs) promote immune responses to foreign Ags and immune tolerance to self-Ags. Deregulation of DCs is implicated in autoimmunity, but the molecules that regulate DCs to protect against autoimmunity have remained unknown. In this study, we show that mice lacking the protein tyrosine phosphatase Shp1 specifically in DCs develop splenomegaly associated with more CD11c$^+$ DCs. Splenic DCs from the mutant mice showed upregulation of CD86 and CCR7 expression and of LPS-induced production of proinflammatory cytokines. The mice manifested more splenic Th1 cells, consistent with the increased ability of their DCs to induce production of IFN-γ by Ag-specific T cells in vitro. The number of splenic CD5$^+$CD19$^+$ B-1a cells and the serum concentrations of Igs M and G2a were also increased in the mutant mice. Moreover, aged mutant mice developed glomerulonephritis and interstitial pneumonitis together with increased serum concentrations of autoantibodies. Shp1 is thus a key regulator of DC functions that protects against autoimmunity. *The Journal of Immunology*, **2012, 188: 5397–5407.**

Dendritic cells (DCs) are professional APCs that play two distinct roles in the immune system: initiation and modulation of the immune responses of T cells to pathogens and induction and maintenance of T cell tolerance to self-components in the periphery (1, 2). For the former role, DCs recognize pathogens or exogenous Ags through pattern recognition receptors such as TLRs and thereby become activated. Such activation is associated with maturation of DCs and upregulation of the expression of MHC class II molecules and of costimulatory molecules such as CD80, CD86, and CD40 on the cell surface. The mature DCs present MHC–antigenic peptide complexes together with costimulatory molecules to naive CD4$^+$ Th cells, which promotes their differentiation into effector Th cells such as IFN-γ–producing Th1 cells, IL-4–producing Th2 cells, and IL-17–producing Th17 cells (2). Activated DCs also secrete various cytokines including IL-12, IL-6, and IL-23, which are thought to be important for regulation of DC activity and differentiation of the effector Th cells. The second role of DCs, promotion of T cell tolerance to self-Ags and harmless foreign Ags, is achieved by various mechanisms including the production of IL-10 or activation of TGF–β (3, 4), induction of the differentiation of regulatory T cells (Tregs) (5, 6), and either promotion of T cell anergy or deletion of effector T cells specific for such Ags (7, 8). Deregulation of either of these two major roles of DCs is thought to give rise to fatal autoimmunity, in which effector T cell responses are directed toward self-Ags. Indeed, constitutive deletion of DCs suppresses the expansion and differentiation of autoreactive T cells in the MRL.*Fas*^{lpr} mouse, a model of systemic lupus erythematosus (SLE) (9), whereas such deletion on a non-autoimmune background elicited autoimmunity, possibly through loss of peripheral T cell tolerance (10). However, the precise contribution of DCs to autoimmunity, as well as the molecules that regulate DCs to protect against autoimmunity, remains to be fully elucidated.

Shp1 is a nonreceptor-type protein tyrosine phosphatase (PTP) that contains two tandem Src homology 2 domains, a single PTP domain, and a C-terminal hydrophobic tail with two tyrosine phosphorylation sites (11, 12). Shp1 is highly expressed in DCs and various hematopoietic cells and plays an inhibitory role in signaling pathways initiated by growth factors or cytokines as a result of its binding to their receptors or to ITIM-containing receptor-like proteins, such as signal regulatory protein α or paired Ig-like receptor B (13–15). Indeed, the mouse mutant motheaten (*me/me*) and its allelic variant, viable motheaten (*me^v/me^v*), which harbor mutations in the Shp1 gene (*Ptpn6*) (16, 17), manifest an

*Laboratory of Biosignal Sciences, Institute for Molecular and Cellular Regulation, Gunma University, Maebashi, Gunma 371-8512, Japan; †Department of Orthopedic Surgery, Gunma University Graduate School of Medicine, Maebashi, Gunma 371-8511, Japan; ‡Department of Medicine and Clinical Science, Gunma University Graduate School of Medicine, Maebashi, Gunma 371-8511, Japan; and §Division of Molecular and Cellular Signaling, Department of Biochemistry and Molecular Biology, Kobe University Graduate School of Medicine, Chuo-ku, Kobe 650-0017, Japan

[1]T. Kaneko, Y.S., and T. Kotani contributed equally to this work.

Received for publication November 10, 2011. Accepted for publication March 26, 2012.

This work was supported in part by a Grant-in-Aid for Scientific Research (B) (to T.M.), a Grant-in-Aid for Young Scientists (B) (to Y.S.), the Support Program for Improving Graduate School Education (to T. Kaneko), and a grant of the Global Center of Excellence Program from the Ministry of Education, Culture, Sports, Science and Technology of Japan.

Address correspondence and reprint requests to Prof. Takashi Matozaki, Division of Molecular and Cellular Signaling, Department of Biochemistry and Molecular Biology, Kobe University Graduate School of Medicine, 7-5-1 Kusunoki-cho, Chuou-ku, Kobe 650-0017, Japan. E-mail address: matozaki@med.kobe-u.ac.jp

The online version of this article contains supplemental material.

Abbreviations used in this article: ANA, anti-nuclear Abs; cDC, conventional dendritic cell; CKO, conditional knockout; DC, dendritic cell; DN, double negative; LN, lymph node; pAb, polyclonal Ab; pDC, plasmacytoid dendritic cell; PDTC, pyrrolidine dithiocarbamate; PI, propidium iodide; PTP, protein tyrosine phosphatase; SLE, systemic lupus erythematosus; Treg, regulatory T cell.

www.jimmunol.org/cgi/doi/10.4049/jimmunol.1103210

enlarged spleen and lymph nodes (LNs) together with increased numbers of myeloid cells, plasma cells, and Mott cells (18–20). In addition, *me/me* and me^v/me^v mice (hereafter both referred to as *motheaten* mice) experience chronic inflammation and systemic autoimmune disease, as evidenced by hypergammaglobulinemia, high titers of autoantibodies, and immune complex deposition with consequent tissue damage (20). As a result, the mutant animals die of interstitial pneumonitis at ~2–3 wk (*me/me*) or 9–12 wk (me^v/me^v) of age (18, 19). The functional abnormality of DCs in *motheaten* mice has remained uncharacterized, but the number of DCs in these animals is markedly increased in lung, liver, and kidney, suggesting a role for Shp1 in negative regulation of DC proliferation and differentiation (21).

It is difficult to distinguish between DC-intrinsic and DC-extrinsic effects of Shp1 deficiency in *motheaten* mice, however, given that the enzyme is ablated in all somatic cells. In addition, examination of the effects of an inhibitor of Shp1 or of RNA interference-mediated knockdown of Shp1 has indicated that Shp1 is an intrinsic but negative regulator of DC functions including the production of proinflammatory cytokines, migration to draining LNs, and the control of many facets of T cell-mediated immune responses (22). The precise role of Shp1 in the regulation of DC functions, especially in vivo, has however remained unclear. To address this issue, we have now generated and analyzed DC-specific Shp1 conditional knockout (CKO) mice.

Materials and Methods

Abs and reagents

A rat mAb to mouse CD16/32 (2.4G2) was prepared from the culture supernatants of hybridoma cells (kindly provided by K. Okumura, Juntendo University, Tokyo, Japan). Rabbit polyclonal antibodies (pAbs) to Shp1 were obtained from Santa Cruz Biotechnology (Santa Cruz, CA). A mouse mAb to β-tubulin (TUB2.1) as well as LPS and FITC isomer I were from Sigma-Aldrich (St. Louis, MO). HRP-conjugated goat pAbs to rabbit or mouse IgG as well as Cy3-conjugated goat pAbs to rat IgG were obtained from Jackson ImmunoResearch (West Grove, PA). A mouse mAb to phosphotyrosine (4G10) was obtained from Millipore (Billerica, MA). Pyrrolidine dithiocarbamate (PDTC), JSH-23, SB203580, wortmannin, and PP2 were obtained from Merck (Darmstadt, Germany). SP600125 or bisindolylmaleimide I was from Wako (Osaka, Japan) or Cell Signaling Technology (Danvers, MA), respectively. FITC-conjugated mAbs to mouse CD8α (53-6.7), CD62L (MEL-14), CD5 (53-7.3), CD4 (RM4-5), and IFN-γ (XMG1.2); PE-conjugated mAbs to mouse IL-17A (TC11-18H10), IL-4 (11B11), B220 (RA3-6B2), CD21/35 (7G6), and Gr-1 (Rb6-8C5); PE- or biotin-conjugated rat IgG to trinitrophenol (isotype control); an allophycocyanin-conjugated mAb to mouse CD11c (HL3); a PE–Cy7–conjugated mAb to mouse CD4 (RM4-5); biotin-conjugated mAb to mouse CD4 (RM4-5) and CD40 (3/23); PE-conjugated streptavidin; and allophycocyanin-conjugated streptavidin were obtained from BD Biosciences (San Jose, CA). FITC-conjugated mouse IgG to trinitrophenol (eBM2a, isotype control) and an mAb to Thy1.2 (30-H12), a PE-conjugated mAb to mouse CD8α (53-6.7), and CD69 (H1.2F3), an allophycocyanin-conjugated mAb to mouse Foxp3 (FJK-16s), and biotin-conjugated mAbs to mouse CD80 (16-10A1), CD86 (GL1), CD70 (FR70), Thy1.2 (30-H12), CD23 (B3B4), CD25 (PC61), TER119 (TER-119), CCR7 (4B12), and MHC class II (M5/114.15.2) were obtained from eBioscience (San Diego, CA). A PE-conjugated mAb to mouse F4/80 (BM8) was from Caltag (Burlingame, CA). An allophycocyanin-conjugated mAb to mouse CD44 (IM7); an allophycocyanin/Cy7-cojugated mAb to mouse B220 (RA3-6B2); PE/Cy7-conjugated mAb to AA4.1; and a biotin-conjugated mAb to mouse CD19 (6D5) and F4/80 (BM8) were obtained from BioLegend (San Diego, CA). Microbeads conjugated with Abs to mouse CD11c (N418) or to CD4 (L3T4) or with anti-biotin were obtained from Miltenyi Biotech (Bergisch Gladbach, Germany). HRP-conjugated (or nonconjugated) goat pAbs to mouse IgA, IgG1, IgG2a, IgG2b, and IgG3 were obtained from Bethyl Laboratories (Montgomery, TX). Rabbit pAbs to mouse IgM and HRP-conjugated goat pAbs to mouse IgM were from Zymed (South San Francisco, CA). Cy3-conjugated goat pAbs to mouse IgG were obtained from Jackson ImmunoResearch. FITC-conjugated rabbit pAbs to C3 were obtained from Abcam (Cambridge, U.K.). RPMI 1640 medium (Sigma-Aldrich) was supplemented with 10% heat-inactivated FCS, 50 μM 2-ME, 2 mM L-glutamine, 10 mM HEPES–NaOH (pH 7.4), penicillin (100 U/ml), streptomycin (100 μg/ml), and 1 mM sodium pyruvate to yield complete medium.

Animals

CD11c-*cre* mice were generated as described previously (23) and were obtained from The Jackson Laboratory (Bar Harbor, ME). They were crossed with $Ptpn6^{fl/fl}$ mice, which were generated as described previously (24), and the resulting $Ptpn6^{fl/fl}$; CD11c-*cre* (Shp1 CKO) descendants and their sex- and age-matched $Ptpn6^{fl/fl}$ littermates (controls) were studied. OT-II TCR transgenic mice ($H\text{-}2^b$), originally generated as described (25), were kindly provided by T. Hirano (RIKEN, Yokohama, Japan). Mice were bred and maintained at the Institute of Experimental Animal Research of Gunma University under specific pathogen-free conditions and were handled in accordance with the animal care guidelines of Gunma University.

Detection of deleted and floxed alleles of Ptpn6 by PCR

Splenocytes were stained with an FITC-conjugated mAb to mouse CD3ε, a PE-conjugated mAb to mouse B220, an allophycocyanin-conjugated mAb to mouse CD11c, an allophycocyanin–Cy7–conjugated mAb to mouse B220, and propidium iodide (PI). $CD11c^{high}B220^-$ conventional dendritic cells (cDCs), $CD11c^{int}B220^+$ plasmacytoid dendritic cells (pDCs), $CD11c^-CD3^+B220^-$ T cells, and $CD11c^-CD3^-B220^+$ B cells were then sorted with the use of the FACSAriaII instrument. The purity of the isolated cells was >98% for cDCs, >91% for pDCs, and >99% for T and B cells, as determined by flow cytometry. Genomic DNA was isolated from each cell population with the use of a DNeasy kit (Qiagen, Valencia, CA). Floxed (~550-bp product) and deleted (~330-bp product) *Ptpn6* alleles were then identified by PCR with SHCP27 (5′-ACCCTCCAGCTCC-TCTTC-3′), SHCP29 (5′-TGAGGTCCCGGTGAAACC-3′), and SHCP32 (5′-TGTTATGCATGTGTGTATCG-3′) primers as described previously (24). The intensities of PCR bands were determined by densitometric analysis with ImageJ software (National Institutes of Health). Deletion efficiency in each cell population was determined as the intensity of the deleted allele expressed as a percentage of that of the floxed allele plus that of the deleted allele.

Immunoblot analysis

For immunoblot analysis, cells were homogenized on ice in a lysis buffer [20 mM Tris-HCl (pH 7.6), 140 mM NaCl, 1 mM EDTA, 1% Nonidet P-40] containing 1 mM PMSF, aprotinin (10 μg/ml), and 1 mM sodium vanadate. The lysates were centrifuged at 10,000 × *g* for 15 min at 4°C, and the resulting supernatants were subjected to SDS- PAGE followed by immunoblot analysis with various Abs. Immunoreactive bands were then detected with an ECL detection system (GE Healthcare, Little Chalfont, U.K.) and an LAS 3000 image analyzer (Fujifilm, Tokyo, Japan). The intensity of bands was determined by densitometric analysis with the use of Image Gauge 4.0 software (Fujifilm).

Cell preparation and flow cytometry

For analysis or preparation of DCs or $F4/80^+$ macrophages from the spleen, peripheral LNs, or thymus (26, 27), tissue was minced with the use of forceps and then digested with collagenase (Wako, Osaka, Japan) at 400 U/ml in the presence of 5 mM EDTA (Sigma) for 30 min at 37°C. The undigested fibrous material was removed by filtration through a 70-μm cell strainer (BD Falcon, San Jose, CA), and RBCs in the filtrate were lysed with Gey's solution. The remaining cells were washed twice with PBS. $CD11c^+$ or $F4/80^+$ cells were further isolated from splenocytes with the use of anti-CD11c microbeads or anti-F4/80 biotin and anti-biotin microbeads and a MACS column (Miltenyi Biotec). The purity of the isolated $CD11c^+$ DCs or $F4/80^+$ macrophages was >95% as determined by flow cytometry.

For analysis of T and B cells in the spleen, the tissue was gently ground with autoclaved frosted glass slides in PBS, and the released cells were exposed to Gey's solution and then washed twice with PBS. For isolation of B cells, splenocytes were incubated consecutively with a biotin-conjugated mAb to CD19 and anti-biotin microbeads and were then fractionated with a MACS column. For isolation of total T cells or $CD4^+$ T cells, splenocytes were filtered through nylon wool. Cells in the filtrate were then incubated either consecutively with a biotin-conjugated mAb to Thy1.2 and anti-biotin microbeads or with anti-CD4 microbeads, respectively, before fractionation with a MACS column. The purity of the isolated B cells, $Thy1.2^+$ T cells, or $CD4^+$ T cells was >95% as determined by flow cytometry.

For flow cytometric analysis, cells were first incubated with an mAb specific for mouse CD16/32 to prevent nonspecific binding of labeled mAbs to FcγRs and were thereafter labeled with specific mAbs. Cells isolated

from each tissue were then subjected to flow cytometry with the use of a FACSCalibur or FACSAriaII instrument (BD Biosciences), and all data were analyzed with FlowJo software (Tree Star, Ashland, OR).

Immunohistofluorescence analysis

The spleen was embedded in OCT compound (Sakura Fine Technical, Tokyo, Japan) and rapidly frozen in liquid nitrogen. Cryostat sections with a thickness of 7 μm were then prepared, fixed with methanol, and stained with an FITC-conjugated mAb to B220 or to Thy1.2 as well as with a biotin-conjugated mAb to CD11c and Cy3-conjugated streptavidin. Conventional fluorescence or bright-field images were acquired with a BX-51 microscope equipped with ×10/0.4 and a ×4/0.16 objective lenses, a DP71 camera (Olympus, Tokyo, Japan), and DP controller software (Olympus) and were processed with Adobe Photoshop 7.0 software (Adobe Systems, San Jose, CA). Quantitative analysis of spleen images or for glomerular pathology was performed by the use of ImageJ software (National Institutes of Health).

Histopathology

Mice were perfused transcardially with 4% paraformaldehyde in PBS, after which tissues were removed, embedded in paraffin, and sectioned for staining with Mayer's H&E. For detection of immune complex deposition, cryostat sections (thickness, 7 μm) of the kidney were prepared, fixed with ice-cold acetone, and stained with a Cy3-conjugated pAb to mouse IgG or with FITC-conjugated pAbs to C3. Conventional fluorescence images were obtained as described earlier.

FITC sensitization

Sensitization of the skin with FITC to determine the migration of cutaneous DCs to draining LNs was performed as described previously (28). In brief, FITC isomer I was dissolved in a 50/50 (v/v) acetone/dibutylphthalate mixture immediately before application. Mice were painted on the shaved thorax and abdomen with 200 μl 1% FITC solution or vehicle alone. After 24 h, the inguinal and axillary LNs were isolated and digested with collagenase as described earlier. Cells were washed and then stained first with a biotin-conjugated mAb to mouse MHC class II and then with PE-conjugated streptavidin. The cells were washed again, stained with PI, and then analyzed by flow cytometry.

Ag uptake and processing

For analysis of the uptake and processing of OVA by DCs, splenic $CD11c^+$ DCs were isolated as described earlier and cultured with DQ-OVA (Invitrogen, Carlsbad, CA) at 100 ng/ml in complete medium for 0 to 120 min at 37°C or 4°C. DQ-OVA is a self-quenched conjugate of OVA that exhibits bright-green fluorescence after its proteolytic degradation. The cells were then washed with ice-cold PBS and analyzed by flow cytometry.

Proliferation of T cells from OT-II mice

For assay of the proliferation of T cells from OT-II mice in vitro (26), 12- to 16-wk-old Shp1 CKO and control mice were injected intravenously with 3 mg OVA (Calbiochem, San Diego, CA). After 12 h, $CD11c^+$ DCs were purified from the spleen and cultured for 72 h at various densities with OT-II $CD4^+$ T cells (1×10^5 cells per well) in 96-well, round-bottom microplates; the final 12 h of culture was performed in the additional presence of [^{3}H]thymidine (TdR) at 1 μCi per well, and the cell-associated radioactivity was subsequently measured with a scintillation spectrometer (Top Count NXT; PerkinElmer, Norwalk, CT). Culture supernatants were also assayed for IFN-γ and IL-17 with ELISA kits (R&D Systems, Minneapolis, MN).

Assay of TLR-induced cytokine production by splenic DCs

$CD11c^+$ cells (1×10^5 per well of 96-well, flat-bottom microplates) isolated from the spleens of 12- to 16-wk-old mice were cultured for 24 h in RPMI complete medium in the absence or presence of LPS (1 μg/ml). Culture supernatants were then assayed for TNF-α, IL-12 (p40), IL-1β, IL-6, IL-10, and IFN-β with ELISA kits (R&D Systems).

Intracellular cytokine staining

The intracellular expression of IL-17, IL-4, and IFN-γ in $CD4^+$ T cells was analyzed as described previously (29) with minor modifications. In brief, splenocytes were cultured for 4 h with PMA (100 ng/ml) and ionomycin (1 μg/ml), with GolgiPlug (BD Biosciences) being added at 1 μg/ml for the last 2 h. The cells were stained consecutively with a biotin-conjugated mAb to CD4 and allophycocyanin-conjugated streptavidin, fixed with 4% paraformaldehyde, and permeabilized with the use of a Cytofix/Cytoperm kit (BD Biosciences). Intracellular cytokine staining was performed with a PE-conjugated mAb to IL-17A or to IL-4 and with an FITC-conjugated mAb to IFN-γ, and the cells were then analyzed by flow cytometry.

Assay of serum Ig, anti-nuclear Abs, and anti-dsDNA

Serum was diluted 1:200 to 1:16,000, added to 96-well flat-bottom microplates coated with Abs to mouse IgM, IgG1, IgG2a, IgG2b, IgG3, or IgA, and allowed to react at 37°C for 2 h. The wells were washed and then incubated with 100 μl of a 1:4000 to 1:80,000 dilution of corresponding HRP-conjugated Abs to mouse IgM, IgG1, IgG2a, IgG2b, IgG3, or IgA at 37°C for 1 h. A tetramethylbenzidine substrate reagent set (BD Pharmingen, San Diego, CA) was used to develop the plates, and the reaction was terminated with stop solution (BD Pharmingen). Absorbance at 450 nm was measured with a microplate reader (MTP-500; Colona Electric, Tokyo, Japan). For measurement of the concentration of anti-nuclear antibodies (ANA) or anti-dsDNA Abs (IgG isotype), serum was diluted 1:100 to 1:500 and assayed with the use of an ANA ELISA kit (Alpha Diagnostics, San Antonio, TX) or anti-dsDNA mouse ELISA kit (Shibayagi, Shibukawa, Japan), respectively.

Statistical analysis

Data are presented as means ± SE and were analyzed with Student *t* test. A p value of <0.05 was considered statistically significant.

Results

Generation of DC-specific Shp1 CKO mice

To examine the impact of Shp1 ablation in DCs, we crossed mice homozygous for a floxed *Ptpn6* allele (24) with mice harboring a transgene for Cre recombinase under the control of the CD11c gene promoter (CD11c-*cre*) (23). Mouse spleen harbors two major subtypes of DCs: $CD11c^{high}$ cDCs and pDCs, the latter of which are defined as $CD11c^{int}B220^+$ cells and produce type I IFNs in response to viral and bacterial pathogens (1, 30). To evaluate the specificity and efficiency of *Ptpn6* deletion in $Ptpn6^{fl/fl}$; CD11c-*cre* (Shp1 CKO) mice at 12–20 wk of age, we isolated genomic DNA from sorted leukocyte populations, including cDCs, pDCs, T cells, and B cells of the spleen, and subjected it to semiquantitative PCR analysis. Consistent with the results of previous studies with the CD11c-*cre* transgene (31, 32), 94 or 79% of $Ptpn6^{fl}$ alleles were deleted in cDCs or pDCs, respectively, of Shp1 CKO mice, whereas only 11 and 4% of the floxed alleles were deleted in T and B cells, respectively (Fig. 1A). Immunoblot analysis also showed that the abundance of Shp1 protein in $CD11c^+$ DCs from the spleen of Shp1 CKO mice was reduced to 10% of that apparent for $Ptpn6^{fl/fl}$ (control) mice, whereas it was not significantly decreased in T, B cells, or $F4/80^+$ macrophages (Fig. 1B). These results thus indicated that the CD11c-*cre* transgene directs both the efficient and specific deletion of the Shp1 gene in $CD11c^+$ DCs.

Importance of Shp1 in DCs for homeostatic regulation of hematopoietic cells in the spleen

Shp1 CKO mice were born apparently healthy, survived to adulthood, and were fertile. They also did not manifest the typical phenotype of *motheaten* mice, characterized by retarded growth, alopecia, and inflammation of the paws (18, 19) (Supplemental Fig. 1). However, Shp1 CKO mice did manifest marked splenomegaly (Fig. 2A). At 12 and 24 wk of age, the weight of the spleen of Shp1 CKO mice was about twice that of the spell of control animals (Fig. 2B). Indeed, the total number of splenocytes as well as the numbers of splenic B cells and $CD4^+$ T cells in Shp1 CKO mice at 10–12 wk of age were also about double those in control mice, whereas the number of splenic $CD8^+$ T cells did not differ significantly between the two genotypes (Fig. 2C). Moreover, the numbers of $F4/80^+$ macrophages, $Gr\text{-}1^+$ granulocytes, and $TER119^+$ erythroblasts in the spleen of Shp1 CKO mice were significantly greater than those in control mice (Fig. 2C), suggesting that the splenomegaly of Shp1 CKO mice is attributable to increased numbers of various cell types.

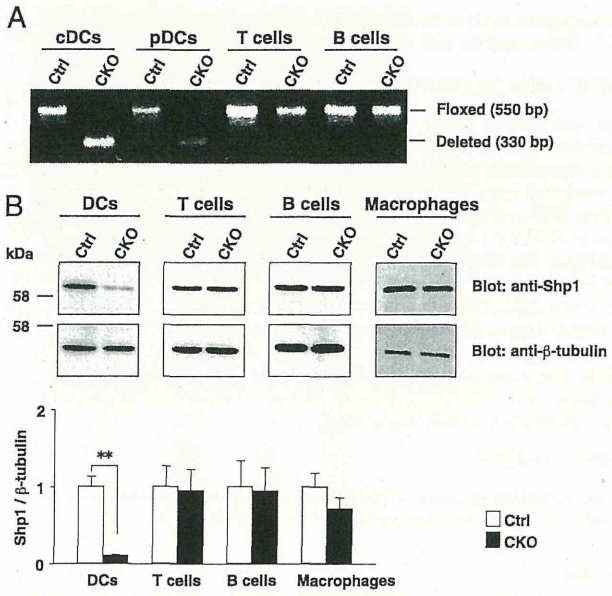

FIGURE 1. Generation of DC-specific Shp1 CKO mice. (**A**) Genomic DNA extracted from cDCs, pDCs, T cells, or B cells sorted from splenocytes of control or Shp1 CKO mice at 12–20 wk of age was subjected to PCR analysis with primers that detect the floxed or deleted alleles of *Ptpn6*. Data are representative of two independent experiments. (**B**) Lysates of DCs, B cells, T cells, or F4/80$^+$ macrophages isolated from the spleen of control or Shp1 CKO mice were subjected to immunoblot analysis with Abs to Shp1 or to β-tubulin (loading control). Blots similar to those shown in the *upper panel* were subjected to densitometric analysis for determination of the ratio of the intensity of the Shp1 band to that of the β-tubulin band (*lower panel*). The quantitative data are expressed relative to the value for control mice and are means ± SE for three mice of each genotype, each of which was examined in an independent experiment. $^{**}p < 0.01$ (Student *t* test). Ctrl, control.

The numbers of both cDCs and pDCs were also markedly increased in the spleen of Shp1 CKO mice at 10–12 wk of age compared with those in the spleen of control mice (Fig. 2D). The cDC population comprises CD4$^+$CD8$^-$ cDCs (CD4$^+$ cDCs), CD4$^-$CD8$^-$ cDCs [double negative (DN) cDCs], and CD4$^-$CD8$^+$ cDCs (CD8$^+$ cDCs) (33, 34). Among these cDC subpopulations, the proportion and the absolute number of DN cDCs in the spleen were markedly increased in Shp1 CKO mice, whereas those of either CD4$^+$ cDCs or CD8$^+$ cDCs were similar for Shp1 CKO and control mice (Fig. 2D). Most CD4$^+$ cDCs and DN cDCs are present in the marginal zone of splenic lymphoid follicles as well as in the marginal zone bridging regions, whereas CD8$^+$ cDCs localize preferentially to the periarteriolar lymphoid sheaths, which are populated mostly by T cells, in the white pulp of the spleen (35). However, immunohistofluorescence analysis revealed that staining for CD11c in the spleen, particularly that in the Thy1.2-positive splenic T cell zones, was greatly increased in Shp1 CKO mice compared with that in the spleen of control mice (Fig. 2E, 2F), suggesting that the distribution of the excess DCs in the spleen of Shp1 CKO mice is disturbed.

In peripheral LNs, the proportion as well as the absolute number of cDCs (but not pDCs) also slightly increased in Shp1 CKO mice at 10–12 wk of age, although such increases were not statistically significant (Supplemental Fig. 2). In contrast, these parameters in the thymus did not differ between Shp1 CKO and control mice at 10–12 wk of age (Supplemental Fig. 2).

Upregulation of DC functions in Shp1 CKO mice

We next examined if the ability of DCs to take up and process Ag might be affected in Shp1 CKO mice. To this end, we incubated purified splenic CD11c$^+$ DCs with DQ-OVA, a self-quenching fluorescently labeled OVA molecule that is degraded to fluorescent peptides after its uptake and intracellular processing (36). We found that neither the uptake nor the processing of DQ-OVA by splenic CD11c$^+$ DCs differed substantially between Shp1 CKO and control mice (Fig. 3A). We next examined the expression of activation markers on CD11c$^+$ DCs under the basal condition. The expression level of CD86 on CD11c$^+$ DCs from the spleen of Shp1 CKO mice at 10–12 wk of age was markedly higher than that for control mice, whereas the expression levels of MHC class II molecules, CD40, and CD80 appeared similar between the two genotypes (Fig. 3B). Moreover, the expression level of CCR7 on splenic CD11c$^+$ DCs of Shp1 CKO mice was substantially higher than that for control mice (Fig. 3B).

We then evaluated the migratory ability of DCs in Shp1 CKO mice. Local application of FITC as a hapten to the skin induces an inflammatory immune response that is studied as a model of contact hypersensitivity (28). It elicits robust migration of DCs in the skin, such as Langerhans cells and dermal DCs, to draining LNs. The total cell number and the number of MHC class II^{high} cells [which represent migratory DCs such as Langerhans cells and dermal DCs from the skin (37, 38)] in the axillary and inguinal LNs did not differ markedly between Shp1 CKO and control mice under the basal condition (data not shown). In contrast, after painting of FITC on the thorax and abdomen, the number of FITC-bearing MHC class II^{high} cells in the LNs of Shp1 CKO mice was significantly increased compared with that apparent for control mice (Fig. 3C), suggesting that the migratory response of skin DCs to FITC painting is upregulated in Shp1 CKO mice.

On activation by pattern recognition receptors such as TLRs, DCs secrete a variety of inflammatory cytokines that are thought to be important for regulation of DC activity and differentiation of effector Th cells (2). We observed that the basal or LPS-induced production of TNF-α, IL-6, IL-1β, and IL-10 by splenic CD11c$^+$ DCs of Shp1 CKO mice was markedly increased compared with that apparent for control mice (Fig. 4A). By contrast, the LPS-induced production of IL-12 (p40) was markedly decreased in CD11c$^+$ DCs from Shp1 CKO mice compared with that apparent for control mice, whereas the basal production of this cytokine did not differ between the two strains (Fig. 4A). In addition, the basal or LPS-stimulated production of IFN-β was also greatly increased in CD11c$^+$ DCs from the spleen of Shp1 CKO mice (Fig. 4A).

To investigate further the molecular mechanism by which Shp1 regulates the LPS-induced production of proinflammatory cytokines, we examined the effects of inhibitors of signaling molecules implicated in this process (39, 40) on the production of IL-6 from splenic DCs of Shp1 CKO mice (Fig. 4B). Treatment with either PDTC or JSH-23, inhibitors of the transcription factor NF-κB (41, 42), markedly decreased IL-6 production from splenic DCs of either Shp1 CKO or control mice in the presence of LPS (Fig. 4B). In addition, treatment with either SB203580 or SP600125, an inhibitor of p38 MAPK or JNK, respectively, also reduced IL-6 production from splenic DCs of either Shp1 CKO or control mice in the presence of LPS (Fig. 4B). In contrast, treatment with wortmannin as an inhibitor of PI3K (Fig. 4B), bisindolylmaleimide I, an inhibitor of protein kinase C, or the Src inhibitor PP2 (data not shown) did not affect the enhanced production of IL-6 by splenic DCs of Shp1 CKO mice. We also examined the abundance of tyrosine-phosphorylated proteins in CD11c$^+$ DCs from the spleen of Shp1 CKO mice. The extent of tyrosine phosphorylation of proteins with molecular masses of ~100 and ~70 kDa was markedly increased in CD11c$^+$ DCs from the spleen of Shp1 CKO mice under either basal or LPS-stimulated conditions compared with that apparent for control mice (Fig. 4C).

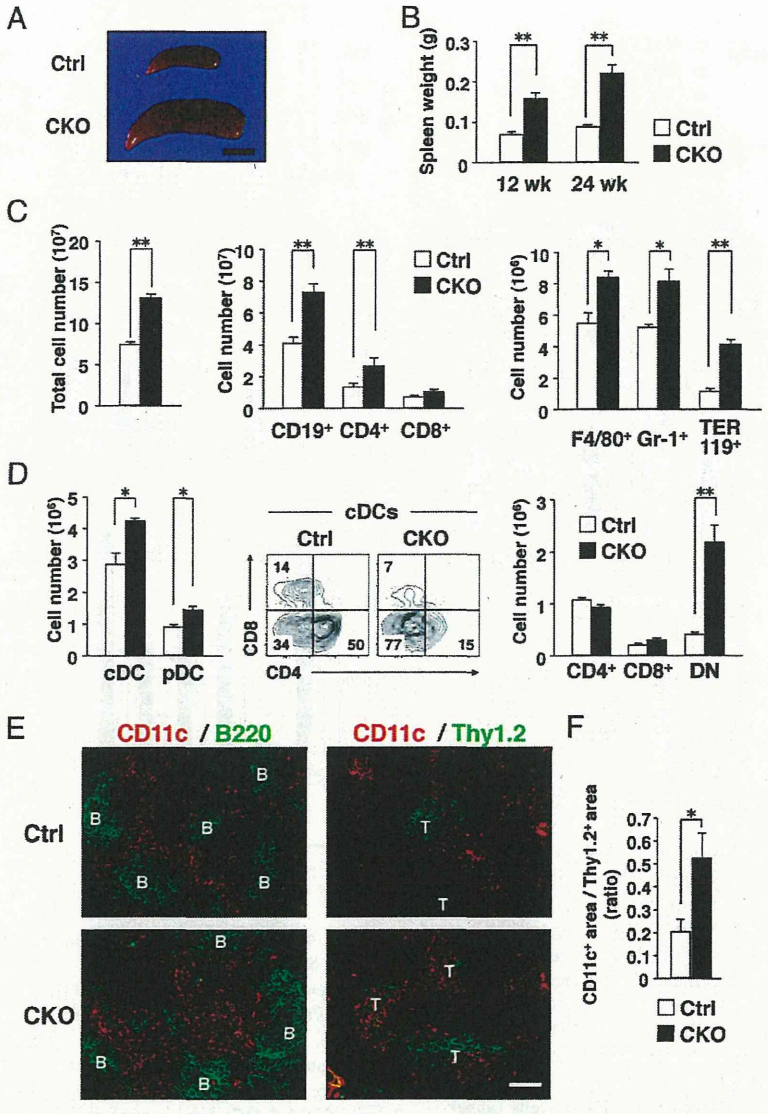

FIGURE 2. Importance of Shp1 in DCs for homeostatic regulation of hematopoietic cells in the spleen. (**A**) Appearance of the spleen of control or Shp1 CKO mice at 26 wk of age. Scale bar, 5 mm. (**B**) Weight of the spleen of control or Shp1 CKO mice at 12 or 24 wk of age. Data are means ± SE from six (12 wk) or five (24 wk) mice per group. $^{**}p < 0.01$ (Student *t* test). (**C**) The total number of splenocytes for control or Shp1 CKO mice at 10–12 wk of age was determined with the use of a Bürker–Türk counting chamber (*left panel*); data are means ± SE for a total of six mice per group analyzed in two independent experiments. The splenocytes were also stained for flow cytometric determination of the absolute numbers of $CD19^+$ B cells, $CD4^+$ T cells, $CD8^+$ T cells, $F4/80^+$ macrophages, $Gr\text{-}1^+$ granulocytes, and $TER119^+$ erythroblasts in PI-negative splenocytes (*middle* and *right panels*); data are means ± SE for three mice per group and are representative of five independent experiments. $^{*}p < 0.05$, $^{**}p < 0.01$ (Student *t* test). (**D**) Splenocytes isolated from control or Shp1 CKO mice at 10–12 wk of age were stained for CD4, CD8, CD11c, and B220 as well as with PI and were then analyzed by flow cytometry for determination of the absolute numbers of $CD11c^{high}B220^-$ cells (cDCs) and $CD11c^{int}B220^+$ cells (pDCs) (*left panel*), the percentages of $CD4^-CD8^+$ ($CD8^+$ cDCs), $CD4^+CD8^-$ ($CD4^+$ cDCs), and $CD4^-CD8^-$ (DN cDCs) cells among cDCs (*middle panel*), and the absolute numbers of $CD4^+$ cDCs, $CD8^+$ cDCs, and DN cDCs (*right panel*), as indicated. Absolute cell numbers are means ± SE for three mice per group and are representative of five independent experiments. $^{*}p < 0.05$, $^{**}p < 0.01$ (Student *t* test). (**E**) Frozen sections of the spleen from control or Shp1 CKO mice at 10–12 wk of age were stained with FITC-conjugated Abs to B220 (green, *left panels*) or to Thy1.2 (green, *right panels*) as well as with biotin-conjugated Abs to CD11c and Cy3-conjugated streptavidin (red). Data are representative of three independent experiments. B and T represent B and T cell areas, respectively. Scale bar, 200 μm. (**F**) By the use of ImageJ software, the Thy1.2-positive area (T cell zone) and the CD11c-positive area in the T cell zone were measured. Data are shown as ratios of the CD11c-positive area to the Thy1.2-positive area. Data are means ± SE for 28 (control mice) and 23 (Shp1 CKO mice) follicles from a total of three mice per group examined in three independent experiments. $^{*}p < 0.05$ (Student *t* test).

High frequency of Th1 cells and increased ability of DCs to promote differentiation of $CD4^+$ T cells into Th1 cells in Shp1 CKO mice

We next examined the effect of Shp1 ablation in $CD11c^+$ DCs on T cell populations in the spleen. The frequency of activated ($CD62L^{low}CD44^{high}$) T cells (43) among either $CD4^+$ or $CD8^+$ T cells was markedly increased in the spleen of Shp1 CKO mice at 20–24 wk of age compared with that for control mice (Fig. 5A), although the frequency of such cells did not differ between the two strains at 10–12 wk of age (data not shown). Moreover, the frequency of IFN-γ–producing $CD4^+$ T cells in the spleen of Shp1 CKO mice at 20–24 wk of age was increased >3-fold compared with that for control mice, whereas the frequency of IL-17– or IL-4–producing $CD4^+$ T cells did not differ between the two genotypes (Fig. 5B). These results indicated that, by 20 wk of age, activation of peripheral T cells and differentiation of $CD4^+$ T cells

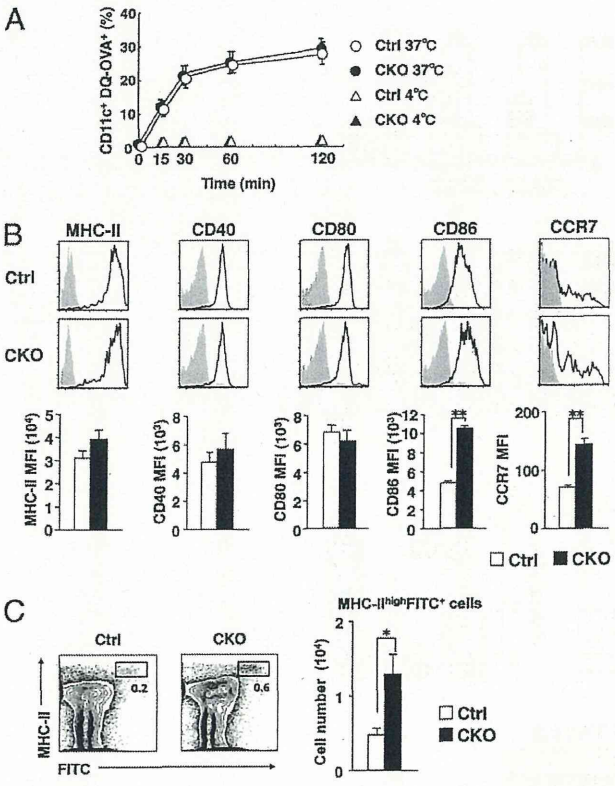

FIGURE 3. Upregulation of DC functions in Shp1 CKO mice. (**A**) Splenic CD11c$^+$ DCs isolated from control or Shp1 CKO mice at 12–16 wk of age were incubated with DQ-OVA (100 ng/ml) for 0–120 min at 37°C or 4°C (negative control), washed, stained with PI, and analyzed by flow cytometry for fluorescent degradation products of DQ-OVA. Data represent the percentage of fluorescence-positive cells among total DCs at each time point; they are means ± SE for three mice per group and are representative of two independent experiments. (**B**) Splenocytes from control or Shp1 CKO mice at 10–12 wk of age were stained for CD11c as well as MHC class II molecules (MHC-II), CD40, CD80, CD86, or CCR7 (open traces), or with isotype control Abs (filled traces), and PI for analysis by flow cytometry. Representative profiles for the expression of MHC class II, CD40, CD80, CD86, or CCR7 on PI-negative CD11c$^+$ cells (*upper panels*) as well as corresponding mean fluorescence intensity (MFI) values (*lower panels*) are shown. MFI data are means ± SE for three mice per group and are representative of three independent experiments. $^{**}p < 0.01$ (Student *t* test). (**C**) Control or Shp1 CKO mice at 12–16 wk of age were painted on the shaved thorax and abdomen with 200 μl 1% FITC. After 24 h, cells were prepared from inguinal and axillary LNs, stained with Abs to MHC class II and with PI, and then analyzed by flow cytometry. The percentage of MHC class II^{high}FITC$^+$ cells among all viable cells on each plot is indicated (*left panel*). The absolute numbers of MHC class II^{high} FITC$^+$ cells were also determined (*right panel*); data are means ± SE for a total of four mice per group examined in two independent experiments. $^*p < 0.05$ (Student *t* test).

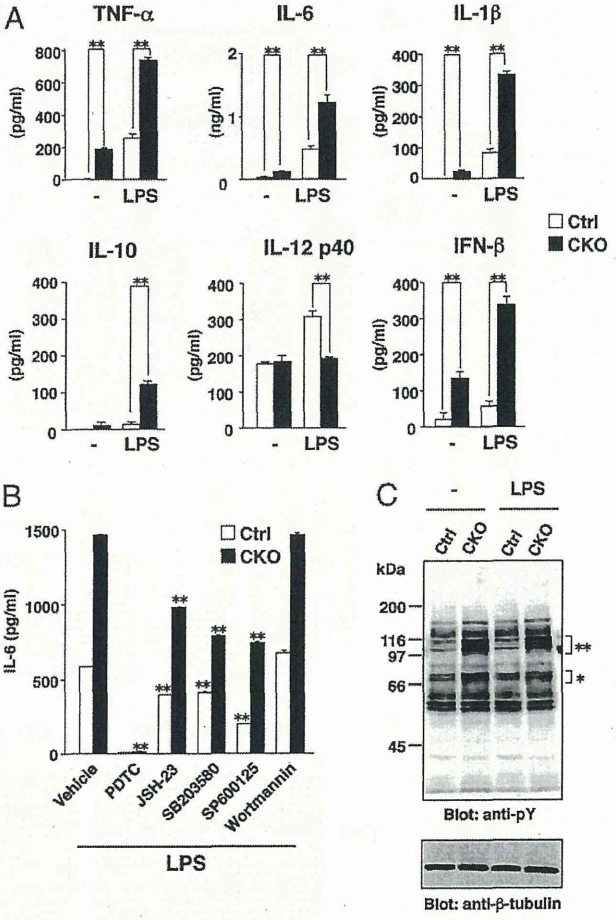

FIGURE 4. Upregulation of proinflammatory cytokine production by DCs from Shp1 CKO mice. (**A**) Splenic CD11c$^+$ DCs from control or Shp1 CKO mice at 12–16 wk of age were cultured in the absence or presence of LPS (1 μg/ml) for 24 h, after which the concentrations of TNF-α, IL-6, IL-1β, IL-10, IL-12 (p40), and IFN-β in culture supernatants were determined. Data are means ± SE of triplicate determinations and are representative of three independent experiments. $^{**}p < 0.01$ (Student *t* test). (**B**) Splenic CD11c$^+$ DCs from control or Shp1 CKO mice were exposed to LPS (1 μg/ml) for 24 h in the absence (vehicle) or presence of the indicated inhibitors of signaling molecules [PDTC (100 μM), JSH-23 (10 μM), SB203580 (10 μM), SP600125 (10 μM), and wortmannin (100 nM)], after which the concentration of IL-6 in culture supernatants was determined. Data are means ± SE of triplicates and are representative of three independent experiments. $^{**}p < 0.01$ (versus the corresponding value for vehicle only in either Shp1 CKO mice or control; Student *t* test). (**C**) Splenic CD11c$^+$ DCs from control or Shp1 CKO mice were exposed to LPS (1 μg/ml) for 15 min, after which cell lysates were prepared and subjected to immunoblot analysis with Abs to phosphotyrosine (pY) or to β-tubulin. Data are representative of three independent experiments. ** and * indicate proteins of ~100 and ~70 kDa, respectively, whose level of tyrosine phosphorylation was increased in CKO mice compared with that in control mice.

toward the Th1 effector lineage were enhanced in Shp1 CKO mice.

We therefore next examined the ability of CD11c$^+$ DCs to promote the Ag-specific proliferation of, as well as the production of IFN-γ by, CD4$^+$ T cells. The proliferation of OVA-specific CD4$^+$ T cells from OT-II mice (25) was increased to a markedly greater extent on culture with OVA-pulsed CD11c$^+$ DCs prepared from Shp1 CKO mice compared with those prepared from control mice (Fig. 5C). Furthermore, the production of IFN-γ, but not that of IL-17, in such cultures was greater with OVA-pulsed CD11c$^+$ DCs of Shp1 CKO mice than with those from control mice (Fig. 5C). These results suggested that the ability of CD11c$^+$ DCs of Shp1 CKO mice to prime and to promote the differentiation of Ag-specific CD4$^+$ T cells to Th1 cells is enhanced compared with that of such cells of control mice.

We also found that the frequency of Foxp3$^+$ Tregs among total CD4$^+$ cells in the spleen was markedly increased for Shp1 CKO mice compared with control mice (Fig. 5D). We also examined the T cell populations in the thymus of Shp1 CKO mice, given that DCs are thought to regulate clonal deletion of self-reactive T cells